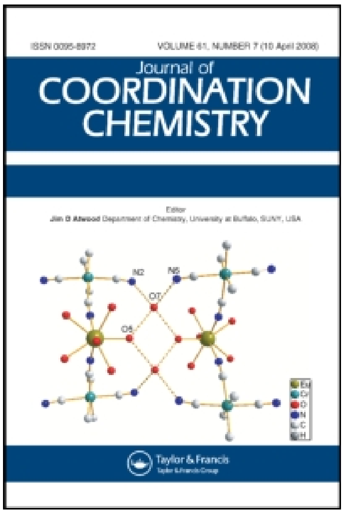

Journal of Coordination Chemistry
Publication details, including instructions for authors and subscription information:
http://www.informaworld.com/smpp/title~content=t713455674

Crystal structures, spectra and magnetic properties of two salts of the bis(maleonitriledithiolato)Ni(III) ion

Mingguo Liu[a]; Chunlin Ni[b]; Chengjiao Mao[c]
[a] College of Chemistry and Life Sciences, China Three Gorges University, Yichang 443002, P.R China [b] Department of Applied Chemistry, College of Science, South China Agricultural University, Guangzhou 510642, P.R China [c] Shayang Teachers' School, Hubei, Jingmen 448200, P.R China

To cite this Article Liu, Mingguo , Ni, Chunlin and Mao, Chengjiao(2006) 'Crystal structures, spectra and magnetic properties of two salts of the bis(maleonitriledithiolato)Ni(III) ion', Journal of Coordination Chemistry, 59: 15, 1775 — 1784

To link to this Article: DOI: 10.1080/00958970600563940

URL: http://dx.doi.org/10.1080/00958970600563940

Journal of Coordination Chemistry
Vol. 59, No. 15, 15 October 2006, 1775–1784

Taylor & Francis
Taylor & Francis Group

Crystal structures, spectra and magnetic properties of two salts of the bis(maleonitriledithiolato)Ni(III) ion

MINGGUO LIU†, CHUNLIN NI*‡ and CHENGJIAO MAO§

†College of Chemistry and Life Sciences, China Three Gorges University, Yichang 443002, P.R. China
‡Department of Applied Chemistry, College of Science, South China Agricultural University, Guangzhou 510642, P.R. China
§Shayang Teachers' School, Hubei Jingmen 448200, P.R. China

(*Received in final form 22 November 2005*)

Two new salts, $[NO_2ClBzPy][Ni(mnt)_2]$ (**1**) and $[NO_2ClBzIQl][Ni(mnt)_2]$ (**2**) ($[NO_2ClBzPy]^+ =$ 1-(2′-nitro-4′-chlorobenzyl)pyridinium, $[NO_2ClBzIQl]^+ =$ 1-(2′-nitro 4′-chlorobenzyl)isoquinolinium, mnt = maleonitriledithiolate) have been prepared and characterized by elemental analyses, IR, MS spectra, single-crystal X-ray diffraction and magnetic susceptibility measurements. Compound **1** is monoclinic, space group $P2_1/n$, $a = 6.913(2)$, $b = 24.524(6)$, $c = 14.199(4)$ Å, $\beta = 101.80(1)^\circ$, $V = 2356.4(11)$ Å^3, $Z = 4$; Compound **2** is triclinic, space group $P\bar{1}$, $a = 7.449(5)$, $b = 10.327(6)$, $c = 17.629(11)$ Å, $\alpha = 106.76(1)$, $\beta = 91.17(1)$, $\gamma = 91.79(1)^\circ$, $V = 1297.3(14)$ Å^3, $Z = 2$. The $Ni(mnt)_2^-$ ions of both **1** and **2** form a 1D zigzag chain through Ni⋯S, S⋯S, Ni⋯Ni and $\pi \cdots \pi$ interactions. Magnetic susceptibility measurements in the temperature range 1.8–300 K show that **1** exhibits antiferromagnetic behaviour with $g = 2.07$, $J = -438.0\,\mathrm{cm}^{-1}$, while **2** is diamagnetic.

Keywords: Maleonitriledithiolate; Pyridinium; Isoquinolinium; Nickel(III); Crystal structure; Magnetic properties

1. Introduction

Maleonitriledithiolate (mnt) salts of Ni, Pd and Pt have been widely investigated due to their application as building blocks in molecular-based materials showing a variety of magnetic, superconducting, and optical properties [1–7]. The discovery in 1996 of the ferromagnetic salt $NH_4 \cdot Ni(mnt)_2 \cdot H_2O$ strongly stimulated studies of mnt complexes with respect to new molecular magnets [8]. Recently, a series of new ion-pair complexes containing benzylpyridinium derivatives ($[RbzPy]^+$) as the counterion for $[M(mnt)_2]^-$ (M = Ni, Pd, or Pt), that exhibit versatile magnetic properties, have been prepared [9–17]. The *quasi*-one-dimensional magnetic properties of these complexes were attributed to segregated columnar stacks of anions and cations, and intermolecular Ni⋯S, S⋯S, Ni⋯Ni or $\pi \cdots \pi$ interactions within the anionic columns.

---

*Corresponding author. Email: scauchemnicl@163.com

Journal of Coordination Chemistry
ISSN 0095-8972 print/ISSN 1029-0389 online © 2006 Taylor & Francis
DOI: 10.1080/00958970600563940

In continuing research on $[M(mnt)_2]^-$ complexes, we have focussed on finding more suitable multifunctional organic cations to tune the crystal stacking of $[M(mnt)_2]^-$ anions with a view to obtaining ideal molecular magnets. Herein, we describe two novel salts, 1-(2′-nitro-4′-chlorobenzyl)pyridinium bis(maleonitriledithiolato) nickel(III), $[NO_2ClBzPy][Ni(mnt)_2]$ (**1**) and 1-(2′-nitro-4′-dichlorobenzyl)isoquinolinium bis(maleonitriledithiolato)nickel(III), $[NO_2ClBzIQl][Ni(mnt)_2]$) (**2**). Spectra, crystal structures and magnetic properties have been investigated.

2. Experimental

2.1. *General materials and techniques*

The starting materials, 1-(2′-nitro-4′-chlorobenzyl)pyridinium bromide ($[NO_2ClBzPy]Br$), 1-(2′-nitro-4′-chlorobenzyl)isoquinolinium bromide ($[NO_2ClBzIQl]Br$) and disodium maleonitriledithiolate (Na_2mnt) were synthesized following literature procedures [18, 19]. A similar method for preparing $[Bu_4N]_2[Ni(mnt)_2]$ was used to prepare $[NO_2ClBzPy]_2[Ni(mnt)_2]$ and $[NO_2ClBzIQl]_2[Ni(mnt)_2]$ [19]. Elemental analyses were run on a Perkin-Elmer 240 instrument. IR spectra were recorded on an IF66V FT-IR (400–4000 cm^{-1}) spectrophotometer using KBr pellets. Electrospray mass spectra were obtained using a Finnigan LCQ mass spectrometer, with a sample concentration ca. 1 mmol dm^{-3}. Magnetic susceptibility data for crushed polycrystalline samples of **1** and **2** were collected over the temperature range 1.8–300 K using a Quantum Design MPMS-5S SQUID magnetometer; data were corrected for diamagnetism of constituent atoms using Pascal's constants.

2.2. *Syntheses*

2.2.1. $[NO_2ClBzPy][Ni(mnt)_2]$)(1). $[NO_2ClBzPy]_2[Ni(mnt)_2]$ (0.838 g, 1.0 mmol) was dissolved in 30 cm^3 of MeCN, then a MeCN solution (10 cm^3) of I_2 (0.150 g, 0.59 mmol) was slowly added. The mixture was stirred for 1 h, and then 80 cm^3 of CH_3OH was added. After the mixture was allowed to stand overnight, 0.513 g of dark microcrystals were filtered off, washed with CH_3OH and Et_2O and dried under vacuum. Yield: 87.2%. Anal. Calcd for $C_{20}H_{10}NiN_6S_4ClO_2$ (%): C, 40.80; H, 1.71; N, 14.27. Found: C, 40.67; H, 2.01; N, 14.11. IR (cm^{-1}): 3089.5s, 3029.6w, 3073.1w, 2202.8s, 1635.3s, 1581.9s, 1569.0s, 1528.9s, 1486.0s, 1449.9s, 1348.9s, 1346.1s.

2.2.2. $[NO_2ClBzIQl][Ni(mnt)_2]$)(2). The procedure for preparing **2** was similar to that for **1**. Yield: 88.5%. Anal. Calcd for $C_{24}H_{12}NiN_6S_4ClO_2$ (%): C, 45.12; H, 1.89; N, 13.16. Found: C, 45.01; H, 2.01; N, 13.05. IR (cm^{-1}): 3090.1s, 3052.5w, 2205.7s, 1647.4s, 1607.2m, 1568.4m, 1525.2s, 1466.7s, 1442.7m, 1395.7s, 1379.0s, 1346.5s.

Single crystals suitable for X-ray structure analyses were obtained by evaporating 1 : 2 (*v*/*v*) MeCN : *i*-PrOH solutions of **1** and **2**.

2.3. *Crystallography*

Intensity data for **1** and **2** were measured on a Smart APEX CCD area detector using graphite-monochromated Mo-Kα radiation ($\lambda = 0.71073$ Å) using the ω scan mode

Table 1. Crystal data and structure refinement detailss for **1** and **2**.

Compound	**1**	**2**
Temperature	293(2)	293(2)
Empirical formula	$C_{20}H_{10}NiN_6S_4ClO_2$	$C_{24}H_{12}NiN_6S_4ClO_2$
Formula weight	588.74	638.80
Wavelength	0.71073	0.71073
Space group	$P2_1/n$	$P\bar{1}$
Unit cell dimensions		
a (Å)	6.913(2)	7.449 (5)
b (Å)	24.524(6)	10.327(6)
c (Å)	14.199(4)	17.629(11)
α (°)		106.76(1)
β (°)	101.80(1)	91.17(1)
γ (°)		91.79(1)
Volume (Å^3), Z	2356.4(11), 4	1297.3(14), 2
Density (calculated) ($g\,cm^{-3}$)	1.660	1.635
Absorption coefficient (mm^{-1})	1.323	1.209
F(000)	1188	646
Crystal size (mm^3)	0.40 × 0.30 × 0.30	0.40 × 0.30 × 0.30
Absorption correction	Empirical (SHELXA)	Empirical (SHELXA)
Max. and min. transmission	0.60 and 0.67	0.65 and 0.70
θ range for data collection (°)	2.93 to 26.96	2.67 to 26.68
Limiting indices	$-8 \le h \le 8$ $-28 \le k \le 19$ $-16 \le l \le 16$	$-8 \le h \le 8$ $-10 \le k \le 12$ $-20 \le l \le 17$
Reflections collected	11411	6309
Independent reflections	4120	4410
R_{int}	0.046	0.021
Refinement method	Full-matrix l-squares on F^2	Full-matrix l-squares on F^2
Goodness-of-fit on F^2	1.019	1.006
Final R indices [$I > 2\sigma(I)$]	$R_1 = 0.0389$, $wR_2 = 0.1025$	$R_1 = 0.0479$, $wR_2 = 0.1165$
Final R indices (all data)	$R_1 = 0.0481$, $wR_2 = 0.1064$	$R_1 = 0.0680$, $wR_2 = 0.1216$
Largest diff. peak and hole [e Å^{-3}]	0.36 and –0.68	0.32 and –0.47

in the range $2.93 < \theta < 26.96$ for **1** and $2.67 < \theta < 26.68$ for **2**. Space groups, lattice parameters, and other relevant information are listed in table 1. The structures were solved by direct methods and refined on F^2 by full-matrix least-squares methods by SHELXTL [20]. All non-hydrogen atoms were refined with anisotropic thermal parameters. H atoms were placed in calculated positions, assigned fixed isotropic displacement parameters 1.2 times the equivalent isotropic U value of the attached atom, and allowed to ride on their respective parent atoms.

3. Results and discussion

3.1. *Structural details*

Compound **1** crystallizes in the monoclinic space group $P2_1/n$ with one $[Ni(mnt)_2]^-$ anion and one 1-(2′-nitro-4′-chlorobenzyl)pyridinium cation in the asymmetric unit. An ORTEP drawing of **1** with the atom labelling is shown in figure 1(a). Selected bond distances, angles and intermolecular Ni $\cdots$ Ni, Ni $\cdots$ S and S $\cdots$ S distances are summarized in table 2. The Ni(III) ion in the $[Ni(mnt)_2]^-$ anion is coordinated by four sulfur atoms of two mnt^{2-} ligands, and exhibits square-planar coordination geometry.

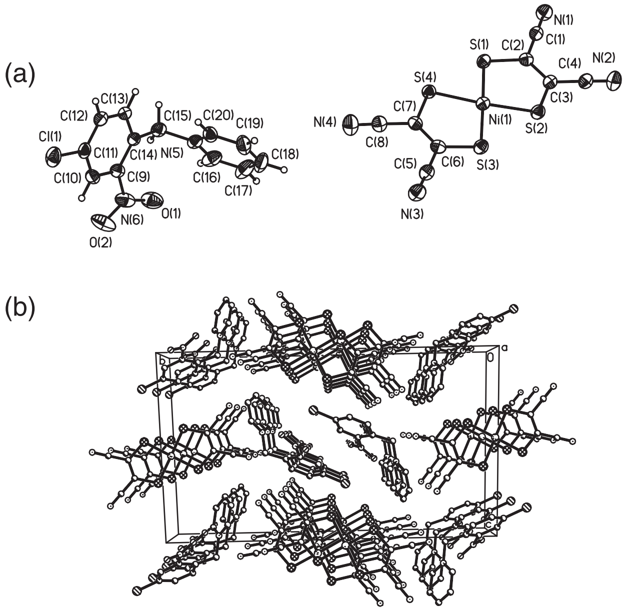

Figure 1. (a) ORTEP plot (30% probability ellipsoids) showing the molecular structure of **1**; (b) packing diagram for **1** viewed along the *a* axis.

Table 2. Selected bond parameters and intermolecular contacts for **1** and **2**.

Compound	**1**	**2**
Bond distances (Å)		
Ni(1)–S(1)	2.144(2)	2.149(2)
Ni(1)–S(2)	2.147(2)	2.128(2)
Ni(1)–S(3)	2.158(2)	2.132(2)
Ni(1)–S(4)	2.144(2)	2.151(2)
S(1)–C(2)	1.704(7)	1.687(5)
S(2)–C(3)	1.701(8)	1.670(5)
S(3)–C(6)	1.716(7)	1.686(5)
S(4)–C(7)	1.723(8)	1.759(5)
Bond angles (°)		
S(1)–Ni(1)–S(2)	92.41(7)	91.89(5)
S(1)–Ni(1)–S(4)	86.44(7)	87.62(5)
S(3)–Ni(1)–S(4)	92.74(7)	93.12(5)
S(2)–Ni(1)–S(3)	88.53(7)	87.38(5)
Intrachain distances (Å)		
Ni $\cdots$ Ni(nearest separation)	3.842, 4.248	3.548, 3.990
Ni $\cdots$ S	3.427, 3.493	3.974, 3.785
S $\cdots$ S	3.789, 3.655	3.540, 3.921

The CN groups are slightly tipped out of the plane, deviations from which plane are 0.0441 Å for N(1), 0.0645 Å for N(2), −0.0073 Å for N(3) and 0.0578 Å for N(4). The average S–Ni–S bond angle in the five-membered rings is 90.03(7)° and the average Ni–S distance is 2.148(2) Å, in agreement with those of previously reported [Ni(mnt)$_2$] complexes [21]. The [NO$_2$ClBzPy]$^+$ cation adopts a conformation in which the benzene and pyridine rings are twisted about the reference plane C(14)–C(15)–N(5) (dihedral angles are 80.6° and 49.3°, respectively). The phenyl and pyridine rings make a dihedral angle of 104.9°. The O atoms of the NO_2 group lie away from the benzene ring plane; deviations from the plane are −0.3868 Å for O(1) and 0.3806 Å for O(2). As shown in figure 1(b), well-segregated columns of anions and cations are stacked along the *a* axis. Within the anion column, Ni(III) ions form a 1D alternating chain through intermolecular Ni···S, S···S, Ni···Ni and $\pi \cdots \pi$ interactions (figure 2a). Adjacent $[Ni(mnt)_2]^-$ anions overlap in two similar ways: pattern A (anion M and A) with Ni···Ni, Ni···S and S···S distances of 3.842, 3.427, and 3.789 Å, respectively (figure 2b), and pattern B (anion M and B) with Ni···Ni, Ni···S and S···S distances of 4.248, 3.493, and 3.655 Å, respectively (figure 2c). In the cation column, there are two interactions found for adjacent cations (figure 3a). One is a hydrogen bond between C(10) on the phenyl ring of a cation and O(2) of a NO_2 group of neighboring phenyl rings (table 3 and figure 3a); the other is a weak p–π interaction between Cl and a neighbouring phenyl ring (the distance between Cl and the centre of the phenyl ring is 3.974 Å). Combination of these interactions generates a cationic column (figure 3b). The closest Ni···Ni separation between anion columns is 12.633 Å, which is significantly longer than the Ni···Ni separations in the chain (3.842 and 4.248 Å). Therefore, **1** can be considered a 1D alternating magnetic chain system from the point of view of its structure. In addition, an intermolecular hydrogen bond between anion and cation is found in the crystal structure of (table 3).

The coordination geometry and stacking pattern for the $[Ni(mnt)_2]^-$ anion in **2** are essentially identical to those described above for **1**, while the overlapping pattern of adjacent anions and the stacking pattern for $[NO_2ClBzIQI]^+$ in **2** are significantly different. As shown in figure 4(a), anions and cations also form segregated columns. Adjacent anions overlap in pattern C (anion M and A, figure 4b) and pattern D (anion M and B, figure 4c); the former is similar to patterns A and B above, but in pattern D two adjacent anions are eclipsed and almost completely overlapped with Ni···Ni and S···S distances of 3.548 and 3.540 Å, respectively. Obviously, the short Ni···Ni, S···S contacts and π–π interactions in **2** are smaller than those in **1**, and it is possible that the interaction between $M(mnt)_2{}^-$ anions in **2** are stronger. For the cation column, adjacent cations are stacked in chair-type conformation and form a 1D chain through π–π stacking involving the isoquinoline rings of neighboring cations; the conjugated electronic system of isoquinoline is larger than that of pyridine (figure 4d) [13]. The reference plane defined by C(14)–C(15)–N(5) and the aromatic rings make dihedral angles of 106.3° for the phenyl ring and 24.5° for the isoquinoline ring. It is worth noting that two intermolecular hydrogen bonds between anions and cations are observed in the crystal structure of **2** as listed in table 3. The anion–anion, anion–cation and cation–cation contacts may play important roles in the stabilization of the lattice of **2**. Selected bond distances, angles, and intermolecular Ni···Ni, Ni···S and S···S distances are summarized in table 2.

3.2. *Infrared and ESI-MS spectra*

IR spectra of **1** and **2** are consistent with the structural data presented above. Bands at 3089, 3030 cm^{-1} for **1** and 3090, 3052 cm^{-1} for **2** are due to aromatic C–H stretching. Complexes **1** and **2** show one strong band at 2203 and 2206 cm^{-1}, respectively, due to

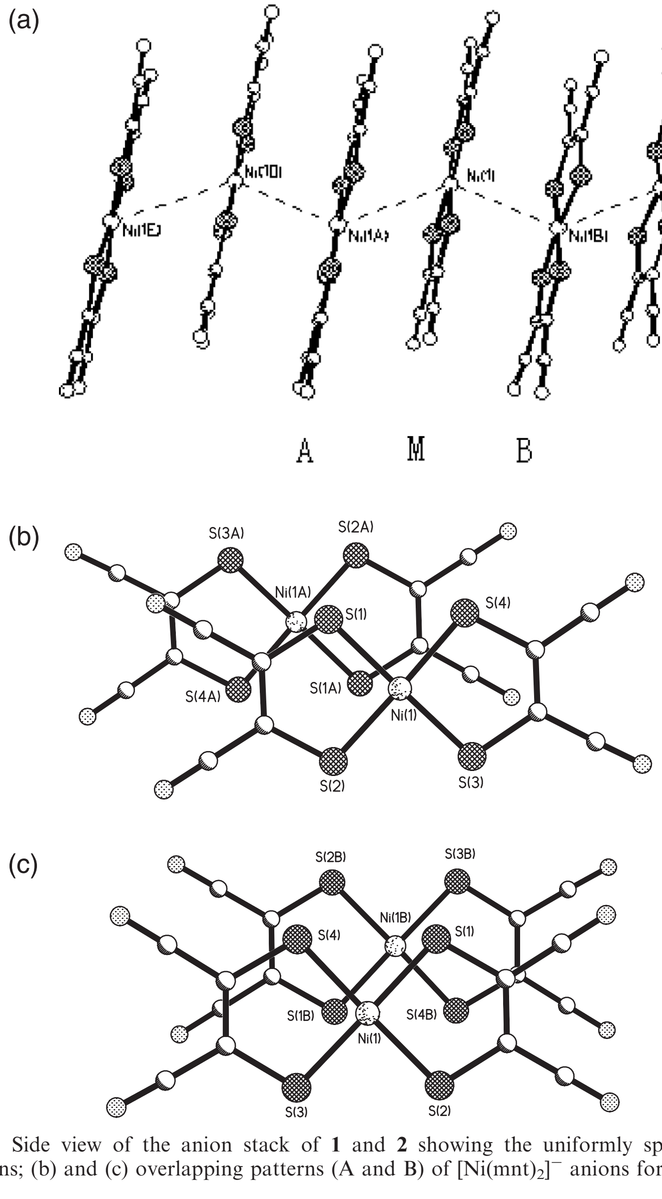

Figure 2. (a) Side view of the anion stack of **1** and **2** showing the uniformly spaced linear chain of $[Ni(mnt)_2]^-$ ions; (b) and (c) overlapping patterns (A and B) of $[Ni(mnt)_2]^-$ anions for **1**.

CN stretching. Bands at 1635, 1582, and 1569 cm^{-1} for **1**, and 1647, 1607, and 1568 cm^{-1} for **2**, are attributable to $\nu(C{=}N)$ and $\nu(C{=}C)$ stretches for the phenyl ring and pyridine (**1**) or isoquinoline (**2**) rings. The $\nu(C{=}C)$ band of mnt^{2-} is at 1450 cm^{-1} for **1** and 1443 cm^{-1} for **2**. The $\nu(NO_2)$ bands of complex **1** and **2** fall at 1529, 1349 cm^{-1}, and 1525, 1346 cm^{-1}, respectively. Negative- and positive-ion ESI-MS spectra of **1** and **2** are dominated by the m/z 340.1 peak, due to $[Ni(mnt)_2{+}H]^-$, and peaks at m/z 249.5 and 299.7 assigned to $[NO_2ClBzPy]^+$ and $[NO_2ClBzIQl]^+$, respectively.

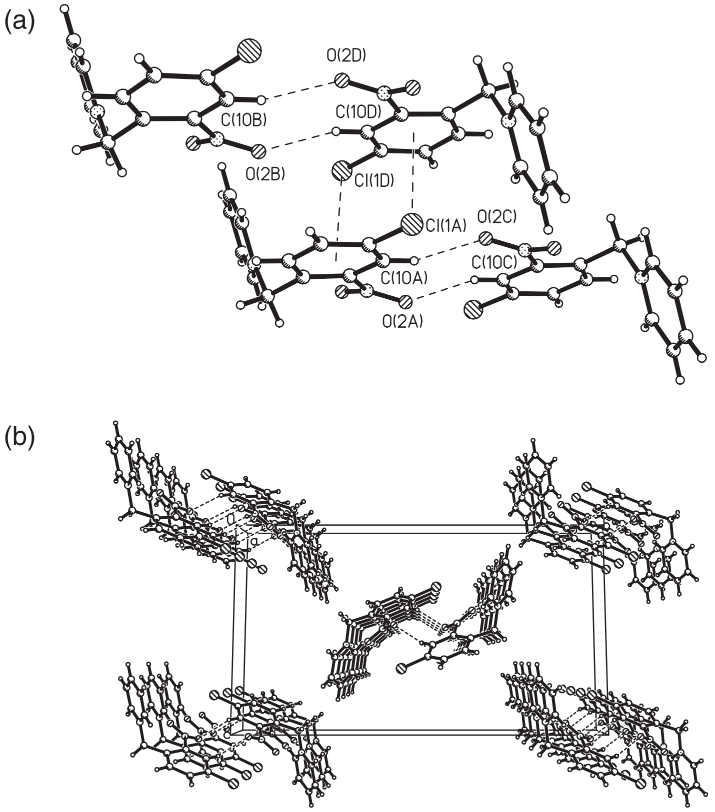

Figure 3. (a) Intermolecular contacts in neighbouring cations of **1**; (b) packing diagram of cations for **1** viewed along the *a* axis.

Table 3. Hydrogen bond data for **1** and **2** (Å and °).

D–H···A	*d* (D–H)	*d* (H···A)	*d* (D···A)	∠(DHA)
1				
C(10)–H(10)···O(2)#1	0.93	2.51	3.398(11)	160.0
C(18)–H(18)···N(1)#2	0.93	2.54	3.404(11)	154.0
2				
C(15)–H(15B)···O(1)#3	0.97	2.59	3.282(6)	128.0
C(23)–H(23)···N(2)#4	0.93	2.61	3.391(8)	141.0

Symmetry transformations used to generate equivalent atoms are #1: $-x+1$, $-y+2$, $-z+2$; #2: $x-1$, $y+1$, z; #3: $x+1$, y, z; #4: $x+1$, y, $z-1$.

3.3. *Magnetic properties*

The temperature dependence of the magnetic susceptibility of **1** and **2** was measured under an applied field of 1000 Oe in the temperature range 1.8–300 K. A plot of $\chi_m T$ *versus* T for **1** is shown in figure 5, where χ_m is the magnetic susceptibility per nickel atom corrected for diamagnetic contributions (-264.9×10^{-6} emu mol^{-1} for **1**). At 300 K, the $\chi_m T$ value for **1** is 0.207 emu K mol^{-1}, which is less than the calculated spin-only value of 0.375 emu K mol^{-1} for a system comprised of non-interacting $g = 2$,

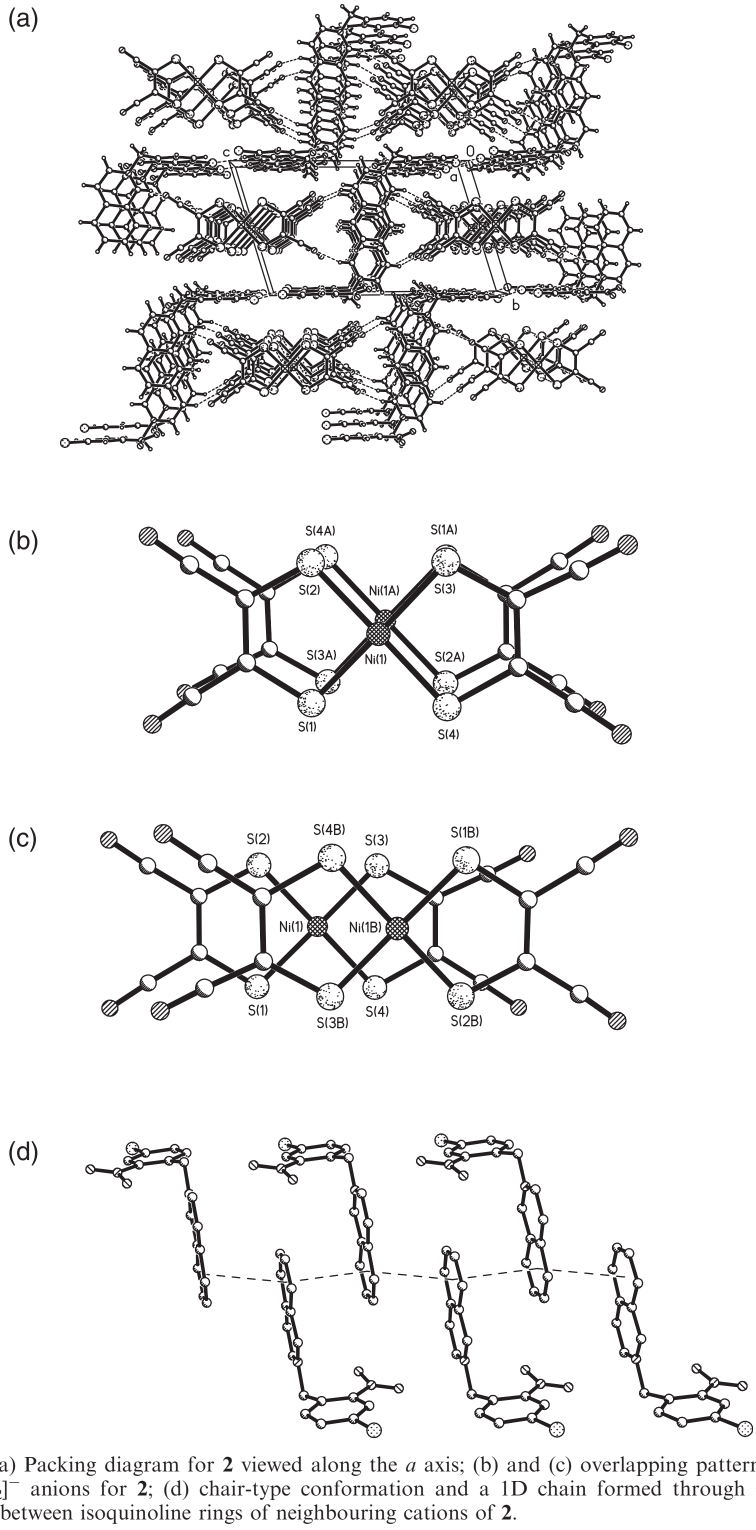

Figure 4. (a) Packing diagram for **2** viewed along the *a* axis; (b) and (c) overlapping patterns (C and D) of $[Ni(mnt)_2]^-$ anions for **2**; (d) chair-type conformation and a 1D chain formed through π–π stacking interactions between isoquinoline rings of neighbouring cations of **2**.

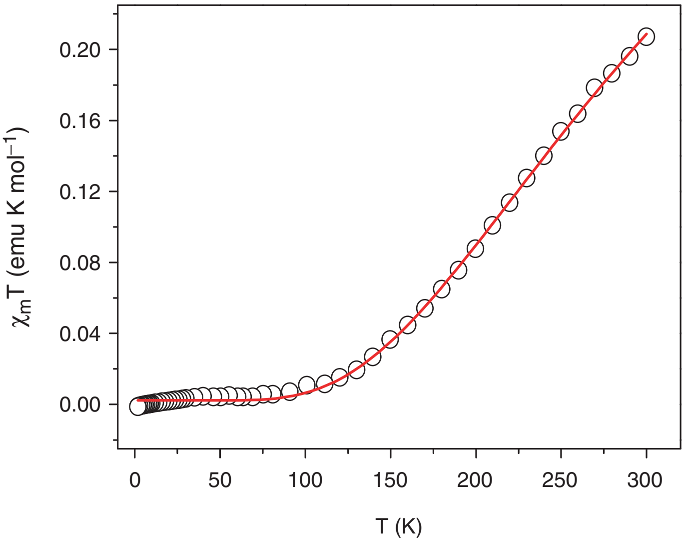

Figure 5. Plot of χ_mT *versus* T for **1**. The solid line is reproduced from theoretical calculations and detailed fitting procedures described in the text.

$S = 1/2$ spin sites, thus indicating that a significant antiferromagnetic coupling contribution is involved. When the system is cooled, the value of χ_mT decreases quickly to 0.0108 emu K mol^{-1} at 100 K, and slowly drops to zero at 1.8 K. Due to the large Ni $\cdots$ Ni distance (4.248 Å), magnetic interactions between nickel(III) ions can be neglected and the magnetic susceptibility data for **1** can be analysed using a simple dinuclear model approximation, the Hamiltonian being $H = 2JS_AS_B$, equation (1) [22],

$$\chi_m = \left(\frac{2N\beta^2g^2}{kT}\right)\frac{(1-\rho)}{(3+\exp(-2J/kT))} + \left(\frac{N\beta^2g^2}{2kT}\right)\rho \tag{1}$$

where N, g, k, β and ρ have their usual meanings, and J is the exchange coupling parameter describing the magnetic interaction between any two neighbouring $S = 1/2$ spins. The best-fit parameters obtained by least-squares fit are $g = 2.07$, $J = -438.0\,\mathrm{cm}^{-1}$, $\rho = 4.0 \times 10^{-3}$ and $R = 4.0 \times 10^{-6}$ ($R = \Sigma(\chi_m\mathrm{T}^{\mathrm{calcd}} - \chi_m\mathrm{T}^{\mathrm{obsd}})^2/\Sigma(\chi_m\mathrm{T}^{\mathrm{obsd}})^2$). The low ρ value suggests that paramagnetic impurities have little effect on the magnetic measurements. The model provides an excellent fit (solid line, figure 5), as indicated by the low value of R.

In the alternating chain of **2**, $[\mathrm{Ni(mnt)_2}]^-$ anions are arranged in the two patterns described above; Ni(1) $\cdots$ Ni(1A) is 3.548 Å, which is significantly larger than that of Ni(1) $\cdots$ Ni(1B). As a consequence, there are strong interactions between Ni(1) and Ni(1A) to form a dimeric structure. Therefore, complex **2** is diamagnetic, as expected.

Supplementary data

Crystallographic data for **1** and **2** have been deposited at the Cambridge Crystallographic Data Centre as supplementary publications. CCDC-280472 and

CCDC-280471, respectively. Copies of the data may be obtained free of charge from The Director, CCDC, 12 Union Road, Cambridge CB2 1EZ, UK (fax: +44-1223-336033; deposit@ccdc.cam.ac.uk or www: http://www.ccdc.cam.ac.uk).

Acknowledgments

The authors thank the President's Science Foundation of the South China Agricultural University (No. 2005K092) for financial support of this work. The Centre for Analysis and Determination of the South China Agricultural University is also acknowledged for its contributions.

References

[1] N. Robertson, L. Cronin. *Coord. Chem. Rev.*, **227**, 93 (2002).
[2] A.E. Pullen, C. Faulmann, K.I. Pokhodnya, P. Cassoux, M. Tokumoto. *Inorg. Chem.*, **37**, 6714 (1998).
[3] J. Nishijo, E. Ogura, J. Yamaura, A. Miyazaki, T. Enoki, T. Takano, Y. Kuwatani, M. Iyoda. *Solid State Commun.*, **116**, 661 (2000).
[4] M. Urichi, K. Yakushi, Y. Yamashita, J. Qin. *J. Mater. Chem.*, **8**, 141 (1998).
[5] P.I. Clemenson, A.E. Underhill, M.B. Hursthouse, R.L. Short. *J. Chem. Soc., Dalton Trans.*, 1689 (1988).
[6] N. Robertson, C. Bergemann, H. Becher, P. Agarwal, S.R. Julian, R.H. Friend, N.J. Hatton, A.E. Underhill, A. Kobayashi. *J. Mater. Chem.*, **9**, 1713 (1999).
[7] J. Nishijo, E. Ogura, J. Yamaura, A. Miyazaki, T. Enoki, T. Takano, Y. Kuwatani, M. Iyoda. *Synth. Met.*, **133–134**, 539 (2003).
[8] A.T. Coomber, D. Beljonne, R.H. Friend, J.L. Brédas, A. Charlton, N. Robertson, A.E. Underhill, M. Kurmoo, P. Day. *Nature*, **380**, 144 (1996).
[9] J.L. Xie, X.M. Ren, Y. Song, Y. Zou, Q.J. Meng. *J. Chem. Soc., Dalton Trans.*, 2868 (2002).
[10] J.L. Xie, X.M. Ren, Y. Song, W.W. Zhang, W.L. Liu, C. He, Q.J. Meng. *J. Chem. Soc., Chem. Commun.*, 2346 (2002).
[11] C.L. Ni, D.B. Dang, Y. Song, S. Gao, Y.Z. Li, Z.P. Ni, Z.F. Tian, L.L. Wen, Q.J. Meng. *Chem. Phys. Lett.*, **396**, 353 (2004).
[12] C.L. Ni, D.B. Dang, Y.Z. Li, S. Gao, Z.P. Ni, Z.F. Tian, Q.J. Meng. *J. Solid State Chem.*, **178**, 100 (2005).
[13] C.L. Ni, Y.Z. Li, D.B. Dang, Y. Song, Z.P. Ni, Q.J. Meng. *Inorg. Chim. Acta*, **358**, 2680 (2005).
[14] J.L. Xie, X.M. Ren, S. Gao, W.W. Zhang, Y.Z. Li, C.S. Lu, C.L. Ni, W.L. Liu, Q.J. Meng, Y.G. Yao. *Eur. J. Inorg. Chem.*, 2393 (2003).
[15] J.L. Xie, X.M. Ren, C. He, Y. Song, Q.J. Meng, R.K. Kremer, Y.G. Yao. *Chem. Phys. Lett.*, **369**, 41 (2003).
[16] X.M. Ren, Q.J. Meng, Y. Song, C.L. Lu, C.J. Hu, X.Y. Chen, Z.L. Xue. *Inorg. Chem.*, **41**, 5931 (2002).
[17] X.M. Ren, Q.J. Meng, Y. Song, C.S. Lu, C.J. Hu. *Inorg. Chem.*, **41**, 5686 (2002).
[18] S.B. Bulgarevich, D.V. Bren, D.Y. Movshovic, P. Finocchiaro, S. Failla. *J. Mol. Struct.*, **317**, 147 (1994).
[19] A. Davison, R.H. Holm. *Inorg. Synth.*, **10**, 8 (1967).
[20] *SHELXTL, Version 5.10. Structure Determination Software Programs*, Bruker Analytical X-ray Systems Inc., Madison, Wisconsin, USA (2000).
[21] K. Brunn, H. Endres, J. Weiss. *Z. Naturforsch.*, **42B**, 1222 (1987).
[22] Y. Song, D.R. Zhu, K.L. Zhang, Y. Xu, C.Y. Duan, X.Z. You. *Polyhedron*, **19**, 1461 (2000).